

SOI PHOTONIC CRYSTAL WAVEGUIDES OPERATING IN TELECOMMUNICATION RANGE FOR INTEGRATED CIRCUITS[#]

Hoang Thi Hong Cam^{1, *}, Trinh Duc Anh¹, Pham Thanh Binh², Pham Van Dai²,
Nguyen Thuy Van², Pham Van Hoi²

¹University of Science and Technology of Hanoi, Vietnam Academy of Science and Technology,
18 Hoang Quoc Viet, Cau Giay, Ha Noi, Viet Nam

²Institute of Materials Science, Vietnam Academy of Science and Technology,
18 Hoang Quoc Viet, Cau Giay, Ha Noi, Viet Nam

*Email: hoang-thi-hong.cam@usth.edu.vn

Received: 15 July 2019; Accepted for publication: 4 September 2019

Abstract: In this report, we present the design and the numerical investigation of the mode property of SOI photonic crystal waveguide (SOI PCWs) operating in telecommunication range, *i.e.*, O-band (1260 – 1360 nm) with TE polarization. The SOI PCWs including conventional W1 and slot SOI PCWs have been designed to exploit two kinds of mode: W1-like and true-slot. For that purpose, the geometric parameters of the SOI PCW with the triangular PhC structure are chosen as follows. The thickness of the silicon slab is fixed at 300 nm, the size of the hole is about 210 nm and the lattice constant is selected of 340 nm. The width of the waveguide is modified from W1 to W1.50 and the width of the slot was selected from 100 nm to 150 nm to engineer the W1-like and true slot modes. The covering material with a refractive index of 1.445 corresponding to some active materials is considered. The demonstrated SOI PCWs in this work might find applications in optical integrated circuits, monitoring or sensing purposes.

Keywords: Silicon-on-insulator, photonic crystal, waveguide, integrated circuit.

Classification numbers: 2.1.1, 2.2.2, 2.4.1.

1. INTRODUCTION

Since it was demonstrated for optical devices in around 2000, silicon photonics has now considered to be a mainstream photonic technology and has played a significant role in optical communications. Silicon photonics is based on silicon-on-insulator (SOI) technology in which devices are fabricated in a layered silicon–insulator–silicon substrate. This platform relies on the high refractive index difference between silicon ($n_{\text{Silicon}} \approx 3.50$ at wavelength of 1360 nm) and buried oxide ($n_{\text{Silica}} \approx 1.445$ at wavelength of 1360 nm) hence the functional optical elements are resided in the thin top silicon core layer. For fabrication techniques, the compatibility of SOI

[#] Presented at the 11th National Conference on Solid State Physics & Materials Science, Quy Nhon 11-2019.

wafers with the complementary metal oxide semiconductor technology and the controlled clean room fabrication processes help silicon photonics to provide tremendous opto-electrical devices. In optical communication, silicon photonics has advantages in supporting low-loss optical waveguiding in sub-wavelength scale because of optical properties of silicon. Silicon has bandgap of around 1.12 eV at room temperature so the optical absorption band edge (cut-off wavelength) is 1100 nm, SOI wafers have high quality of crystalline structure and a good silica/silicon interface. Therefore, SOI platform offers low loss optical guiding structures operating in the optical communication wavelength range, *i.e.* from 1260 nm to 1675 nm. It also has been dominant for fabricating passive and active (optoelectronic) integrated devices [1].

During its development, silicon photonics can contribute various kind of photonic elements, including passive devices [2-4] and active devices [5-9]. It is definitely potential to obtain densely fabricated photonic integrated circuits on a large SOI wafer. Among SOI components towards the integrated optoelectronic circuits, waveguides have been considered to be the most fundamental and basic units and have been of great interest to manipulate the optical modes and improve guiding efficiency.

In term of guiding kinds, silicon photonics can provide various guiding approaches, from simple structures like strip waveguides in which the modes are properly guided in the silicon core area within the submicron sizes [10], to slot waveguides – proposed by Almeida *et al.* [11] by introducing a slot inside the middle of a silicon wire consisting of two strips made of high-index material that enclose a sub-wavelength low-index slot region. In the slot waveguide, the mode is partly confined within the low-index material slot due to the continuities of the normal components of the electric displacement field at the high-index-contrast interfaces between silicon and the low-index material filling the slot. Light can be guided also in bends [3] and micro-ring resonators [12] which are curved and closed loop resonator waveguides. Great effort has been contributed to optimize these structures to achieve low loss. Silicon-based waveguides then extended to photonic crystal (PhC) waveguides, formed by removing one row of holes in the 2-dimensional planar PhC lattice, thus they are named “W1 Photonic crystal waveguides (W1 PCWs)”. Light can be guided along the defect line thanks to the defect states located in the photonic band-gap, *i.e.* the forbidden frequency range in a certain direction for a certain polarization. Interestingly, for these waveguides, light can be even slowed down by engineering flat dispersion. The typical quantity is characterized by group velocity v_g ($v_g = (d\omega/dk)$) which is significantly smaller than the speed of light c in vacuum. The flexibility of the guided modes as well as the slow light behaviors make PCWs interesting for study on slow light [13] or dispersion engineering [14]. In another approach, the mode is guided as the result of the combination of the photonic crystal and the slot effect. Slot PhC waveguides (SPCWs), first introduced by Di Falco *et al.* [15], are created by conducting a groove in the direction of light propagation of the PCWs. When the slot is inserted in the PCWs, the effective index of the structure is reduced, hence not only the W1 mode in conventional W1 PCWs, but also a slot mode occurs. In these structures, the guided modes can be either W1-like mode or true-slot mode. The light is guided and confined in case its electrical field aligns perpendicularly to the slot. The strength of this structure relies on the slow light effects combined with the slot infiltrated with a low-index material, due to the fact that light is strongly confined in the slot regime. Furthermore, the slot can provide space to be filled with an active material that helps to compensate some drawbacks of silicon such as no Pockels effect due to its centrosymmetric crystal structure, strong two-photon absorption in telecommunication range which restricts the ability to exploit third-order nonlinearity in silicon. Hybrid silicon integration has also been paid attention to target further applications besides abusing benefit of silicon.

In this work, we focus on designing the W1-like mode as well as true-slot mode of SOI PCWs operating in telecommunication ranges (e.g., O-band) to exploit the TE-transverse electric field even mode for strengthening light-matter interaction when being filled with an active material to achieve full integrated circuits.

2. DESIGN OF SOI PHOTONIC CRYSTAL WAVEGUIDES

Figure 1 illustrates a SPCW with a cladding material. As we can see in Figure 1(a), one row of the hole is removed and a slot is introduced along the length of the waveguide. The horizontal view of this SPCW is shown in Figure 1(b) with basic parameters: lattice constant a , hole diameter $2r$, width of waveguide W and slot width W_{slot} in the case of SPCW.

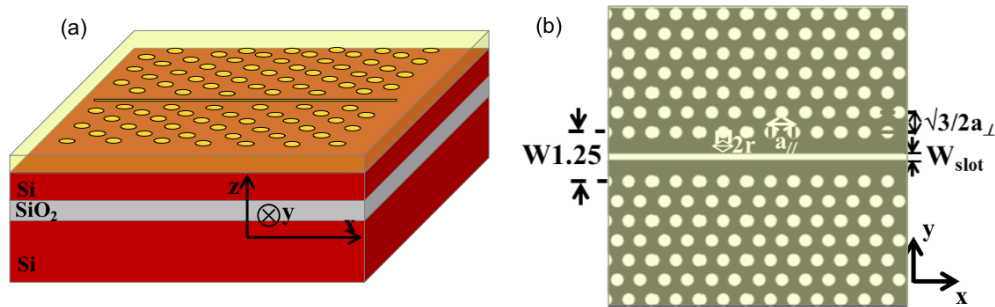


Figure 1. (a) Three-dimensional scheme, and (b) Top view of a cladding material-filled SOI SPCW.

In order to design the proposed SOI PCWs structures, photonic bandgap of planar photonic crystal is first calculated then the dispersion diagram of the SPCWs will be generated by using MIT Photonic Bandgap (MPB) package to serve the 3D Plane Wave Expansion (PWE) method. We aim to manipulate the guiding modes at the O-band, i.e., (1260 – 1360 nm) with TE polarization.

For that intention, the geometry of SOI planar was chosen with the lattice constant of 340 nm, the thickness of silicon core layer of 300 nm which is reasonable for industrial fabrication condition [16, 17], hole diameter of 210 nm, the cladding material with refractive index of 1.0 for air and 1.445 have been considered to study the evolution of photonic band-gap from air hole to material-filled hole. We remind here the refractive index of silicon $n_{Silicon} \approx 3.50$ and silica $n_{Silica} \approx 1.445$ at wavelength of 1360 nm.

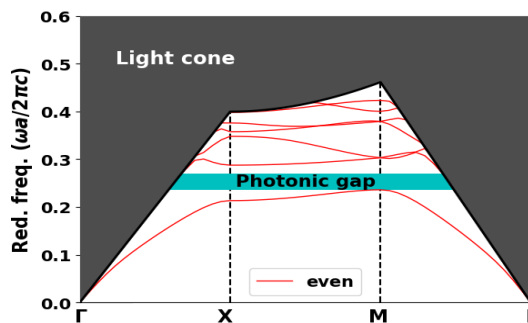


Figure 2. Band diagram for SOI PhC in which lattice constant $a = 340\text{nm}$, hole diameter $2r = 210\text{ nm}$, slab thickness $h = 300\text{ nm}$ and the cladding material has the refractive index of 1.445. The light cone is in gray region, in which the extended modes are located. Below the light line, the TE-like guided bands are localized to the slab: a TE-like gap is present from $\omega = 0.2360$ to $0.2703 (2\pi c/a)$.

Figure 2 presents the TE photonic band-gap of SOI PhC with lattice constant $a = 340$ nm, hole diameter $2r = 210$ nm, slab thickness $h = 300$ nm. For the air cladding, the photonic band-gap is $0.2390 - 0.3190$ in reduced frequency ($2\pi c/a$) unit, *i.e.* $1065.8 - 1422.5$ nm in wavelength range. In the case of material cladding, the photonic band-gap decreases down to $0.2360 - 0.2703$ ($2\pi c/a$) which corresponds to the wavelength range of $1257.9 - 1440.7$ nm. The light cone (grey shaded region) is defined as the area where all the modes which are localized above the light line can leak vertically, leading to intrinsic losses, while below the light line, the modes are properly propagated inside the slab and are evanescent or decaying in an exponential way above and below the slab. We can see the decrease of the photonic band-gap when the cladding environment changes from air to material. The gap reduction from around 355 nm to around 183 nm is caused by the refractive index contrast decrease. From the investigation on the characteristic of photonic band-gap of SOI PhC structure, defects can then be brought into the planar PhC lattice to generate SOI PhC waveguides with the active material cladding of 1.445 refractive index for two guiding structures, W1 PhC waveguides, and slotted ones.

3. RESULTS AND DISCUSSION

3.1. Photonic crystal waveguides

When one row of the hole is removed, the W1 PhC waveguide is created, the width of the waveguide for this standard PCW is $W1 = \sqrt{3}a$. Because the effective index of this structure is larger compared with the planar PhC structure, it supports light confinement by these two following mechanisms: both the total internal reflection and photonic band-gap mechanisms [18-21]. Figure 3(a) depicts the dispersion diagram of this generated W1 PCW. The gray-shaded domain corresponds to the light cone. The black curve package represents the projected slab modes and the two modes in the gap above this package occurring in the photonic band-gap of planar PhC slab are the W1 waveguide modes (the red and green curves as shown in Figure 3(b)) with their E_y profile in insets and the geometry of this PCW is illustrated in Figure 3(c) for the dielectric constant distribution.

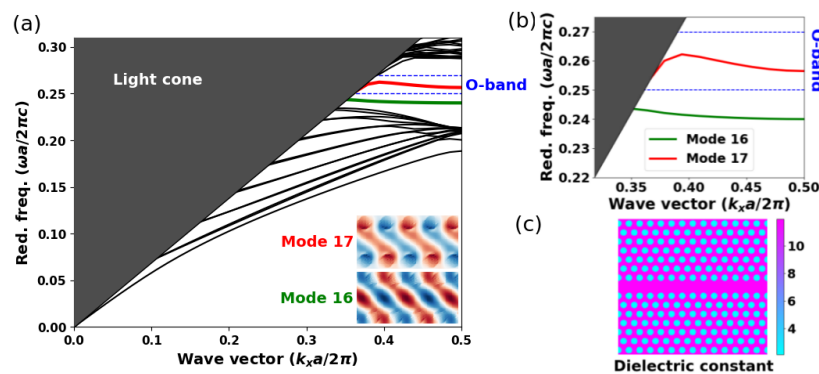


Figure 3. (a) Dispersion diagram of a W1 PCW in which the thickness of silicon slab $h = 300$ nm, lattice constant $a = 340$ nm and the hole diameter $2r = 210$ nm, considering the top cladding material of 1.445 refractive index (insets correspond to the E_y field profiles). (b) Zoom in part of (a) with two W1 TE-like modes: green curve and red curve. (c) Top view of a cladding material-filled SOI PCW.

In addition, apparently these two-guided W1 modes are localized inside the photonic band-gap of the planar PhC in which the upper guided mode resides in the O band with the value of

edge wavelength is around 1325.5 nm (reduced frequency of 0.2565 ($2\pi c/a$)), the lower mode has the edge wavelength of approximately 1416.8 nm (reduced frequency of 0.2399 ($2\pi c/a$)).

3.2. Slot photonic crystal waveguides

In the case of SPCW, as mentioned above, the true-slot mode also appears besides the W1-like mode. This structure exhibits strong potential for light-matter interactions [22-24]. Figure 4 shows the dispersion diagram (Figure 4(a) and (b)) and the structure of SPCWs (Figure 4(c)). Figure 4(a) presents the dispersion diagram of the SPCW in which the slot width is $W_{slot} = 100$ nm and the width of waveguide is $W1.2 = 1.2\sqrt{3}a$. When the slot is inserted to the structure, the effective index of the waveguide structure is reduced so the waveguide has been enlarged to 1.2, *i.e.*, $1.2\sqrt{3}a$ in order to manipulate the W1-like mode as the guided mode in the O-band telecommunication range similar to the case of PCW. As a result, two W1-like modes are present in the O-band range as depicted in Figure 4(a) (red curve and green curve). The edge frequency of the upper guided mode is 0.2612 ($2\pi c/a$), corresponding to the wavelength of 1301.7 nm and the frequency of the lower one is 0.2496 ($2\pi c/a$), corresponding to the wavelength of 1361.0 nm. Regarding the electric field distribution, it is also shown that the electric field is well confined in the slot area for the upper guided mode (red curve) while the electric field distributes also in the two first rows of hole beside the slot as well as the slot for the lower guided mode (green curve).

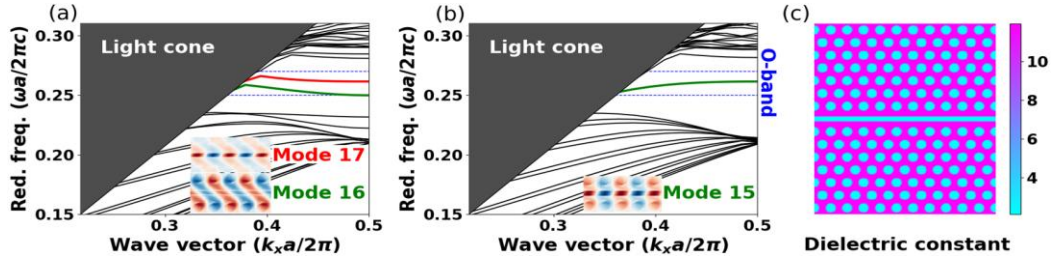


Figure 4. Dispersion diagram of (a) W1.2 SPCW (*i.e.* $1.2\sqrt{3}a$), the slot width $W_{slot} = 100$ nm and (b) W1 SPCW, the slot width $W_{slot} = 140$ nm with the thickness of silicon core slab $h = 300$ nm and the size of material-filled hole $2r = 210$ nm while considering a 1.445 refractive index cladding material (insets correspond to the E_y field profiles). (c) Top view of a cladding material-filled SOI SPCW.

In order to manipulate the true-slot mode, that lies deep below the package of slab modes, the principle is to reduce the effective index by enlarging the size of the slot because the true-slot mode is accounted by the fundamental slot mode projected into the band-gap [15]. In this configuration, the width of waveguide is the same as the normal PCW we studied earlier, *i.e.* $W1 = \sqrt{3}a$ and in order to achieve the true-slot mode operating in the O-band, the slot width is enlarged to 140 nm. By engineering the geometry, the true-slot mode with the edge frequency of 0.2613 ($2\pi c/a$) (the edge wavelength is 1301.2 nm) has been designed and the electric field profile is mapped as shown in Figure 4(b). The electric field is mainly confined in the slot region and the two rows of the hole along the slot. Moreover, it is noticed that the dispersion curve of true-slot mode has positive slope behavior while the W1-like mode has negative slope. The two modes can be manipulated by engineering the geometry properties of the SPCW corresponding to the refractive index of different covering materials, in here, the material of refractive index 1.445 is considered. In addition, the fraction of electric energy confined in slot region can be achieved in the range of 10% - 22%, which is reasonable for hybrid light-matter interaction. This

behavior enables this structure to be employed for combining with active materials such as graphene, quantum dots, semiconducting single-walled carbon nanotubes for further applications besides a guiding device.

4. CONCLUSIONS

In this research, different kinds of modes, *i.e.* W1-like mode and true-slot mode in the SOI PCW and the SPCW have been designed to operate in the O-band of the telecommunication range with the TE polarization. The guided modes have been engineered in the triangular planar lattice with the lattice constant of 340 nm, the silicon core thickness of 300 nm to the suite with the industrial fabrication condition, the hole diameter of 210 nm and the cladding material has refractive index of 1.445 which corresponds to active materials. The fraction of electric field confinement in the slot region can be obtained to 22% by manipulating the width of the slot and the waveguide. These modes of SOI PCWs can be exploited in optical integrated circuits and hybrid light-matter interaction. The dependence of the dispersion on geometry such as the width of the waveguide and slot width as well as the refractive index of covering material provides a general guide line for guiding signals and monitoring or sensing applications.

Acknowledgements. This research is funded by Vietnam National Foundation for Science and Technology Development (NAFOSTED) under grant number 103.03-2017.335.

REFERENCES

1. Vivien T L. and Pavesi L. - Handbook of Silicon Photonics, Taylor & Francis (2013).
2. Selvaraja S. K., Murdoch G., Milenin A., Delvaux C., Ong P., Pathak S., Vermeulen D., Sterckx G., Winroth G., Verheyen P., Lepage G., Bogaerts W., Baets R., Van Campenhout J., and Absil P. - Advanced 300-mm Waferscale Patterning for Silicon Photonics Devices with Record Low Loss and Phase Errors, in 17th Opto-Electronics and Communications Conference Technical Digest (2012) 15–16.
3. Vlasov Y. A. and Mcnab S. J. - Losses in single-mode silicon-on-insulator strip waveguides and bends, *Opt. Express* **12** (8) (2004) 1622–1631.
4. Dai D., Wang J., and Shi Y. - Silicon mode (de)multiplexer enabling high capacity photonic networks-on-chip with a single-wavelength-carrier light, *Opt. Lett.* **38** (9) (2013) 1422–1424.
5. Xu Q., Manipatruni S., Schmidt B., Shakya J., and Lipson M. - 12.5 Gbit/s silicon micro-ring silicon modulators, *Opt. Express* **15** (2) (2007) 430–436.
6. Liu A., Liao L., Rubin D., Nguyen H., Ciftcioglu B., Chetrit Y., Izhaky N., and Paniccia M. - High-speed optical modulation based on carrier depletion in a silicon waveguide, *Opt. Express* **15** (2) (2007) 660–668.
7. Gardes F. Y., Thomson D. J., Emerson N. G., and Reed G. T. - 40 Gb/s silicon photonics modulator for TE and TM polarisations, *Opt. Express* **19** (12) (2011) 11804–11814.
8. Samani A., Chagnon M., Patel D., Veerasubramanian V., Ghosh S., Osman M., Zhong Q., and Plant D. V. - A low-voltage 35-GHz silicon photonic modulator-enabled 112-Gb/s transmission system, *IEEE Photonics J.* **7** (3) (2015) 7901413.

9. Sih V., Xu S., Kuo Y.-H., Rong H., Paniccia M., Cohen O., and Raday O. - Raman amplification of 40 Gb/s data in low-loss silicon waveguides, *Opt. Express* **15** (2) (2007) 357–362.
10. Selvaraja S. K., De Heyn P., Winroth G., Ong P., Lepage G., Cailler C., Rigny A., Bourdelle K. K., Bogaerts W., Van Thourhout D., Van Campenhout J., and Absil P. - Highly uniform and low-loss passive silicon photonics devices using a 300mm CMOS platform, in *Conference on Optical Fiber Communication, Technical Digest Series* (2014).
11. Almeida V. R., Xu Q., Barrios C. A., and Lipson M. - Guiding and confining light in void nanostructure, *Opt. Lett.* **29** (11) (2004) 1209.
12. Zhang W., Serna S., Le Roux X., Alonso-Ramos C., Vivien L., and Cassan E. - Analysis of silicon-on-insulator slot waveguide ring resonators targeting high Q-factors, *Opt. Lett.* **40** (23) (2015) 5566.
13. Schulz S. A., O’Faolain L., Beggs D. M., White T. P., Melloni A., and Krauss T. F. - Dispersion engineered slow light in photonic crystals: a comparison, *J. Opt.* **12** (2010) 104004.
14. Mazoyer S., Hugonin J. P., and Lalanne P. - Disorder-induced multiple scattering in photonic-crystal waveguides, *Phys. Rev. Lett.* **103** (2009) 63903.
15. Di Falco A., O’Faolain L., and Krauss T. F. - Photonic crystal slotted slab waveguides, *Photonics Nanostructures - Fundam. Appl.* **6** (2008) pp. 38–41.
16. <https://www.soitec.com/en/products/photonics-soi/>, Fri. 16 Aug. 2019.
17. <https://www.svmi.com/silicon-wafers/silicon-insulator-wafers/>, Fri. 16 Aug. 2019.
18. Chutinan A. and Noda S. - Waveguides and waveguide bends in two-dimensional photonic crystal slabs, *Phys. Rev. B* **62** (7) (2000) 4488–4492.
19. Notomi M., Shinya A., Yamada K., Takahashi J., Takahashi C., and Yokohama I. - Singlemode transmission within photonic bandgap of width-varied single-line-defect photonic crystal waveguides on SOI substrates, *Electron. Lett.* **37** (5) (2001) 293–295.
20. Baba T., Motegi A., Iwai T., Fukaya N., Watanabe Y., and Sakai A. - Light propagation characteristics of straight single-line-defect waveguides in photonic crystal slabs fabricated into a silicon-on-insulator substrate, *IEEE J. Quantum Electron.* **38** (2) (2002) 743–752.
21. Kuramochi E., Notomi M., Hughes S., Shinya A., Watanabe T., and Ramunno L. - Disorder-induced scattering loss of line-defect waveguides in photonic crystal slabs, *Phys. Rev. B - Condens. Matter Mater. Phys.* **72** (2005) 161318.
22. Di Falco A., O’Faolain L., and Krauss T. F. – Dispersion control and slow light in slotted photonic crystal waveguides, *Appl. Phys. Lett.* **92** (2008) 083501.
23. Serna S., Zhang W., Hoang T. H. C., Alonso-Ramos C., Marris-Morini D., Vivien L., and Cassan E. - Mode selection and dispersion engineering in bragg-like slot photonic crystal waveguides for hybrid light–matter interactions, *Photonics Res.* **6** (1) (2018) 54–60.
24. Prakash C., Sen M., Mondal H., and Goswami K. - Design and optimization of a TE-pass polarization filter based on a slotted photonic crystal waveguide, *J. Opt. Soc. Am. B* **35** (8) (2018) 1791-1798.